Meteoritics & Planetary Science 32, 61–70 (1997)

In situ formation of palisade bodies in calcium, aluminum-rich refractory inclusions

STEVEN B. SIMON[1]* AND LAWRENCE GROSSMAN[1,2]

[1]Department of the Geophysical Sciences, The University of Chicago, 5734 South Ellis Avenue, Chicago, IL 60637, USA
[2]Enrico Fermi Institute, The University of Chicago, 5640 South Ellis Avenue, Chicago, IL 60637, USA
*Correspondence author's e-mail address: sbs8@midway.uchicago.edu

(Received 1996 June 7; accepted in revised form 1996 September 20)

Abstract–It has been suggested that palisade bodies—shells of spinel found within some calcium, aluminum-rich inclusions (CAIs) and the phases the shells enclose—are intact mini-CAIs that predate and were captured by their current hosts while the latter were still molten. We present new data and observations that indicate that most palisade bodies formed instead *in situ* while their host inclusions were crystallizing. The evidence includes observations of spinel-lined cavities and glass-filled, circular structures outlined by spinel in experimental run products crystallized from melts; a partially formed palisade body in an inclusion; a fassaite crystal that is optically continuous across a palisade wall; and similarity of unusual mineral compositions in some palisade bodies and their hosts. Our observations can be used to refute arguments for exotic origin and are most consistent with a model for *in situ* formation involving: (1) formation of vesicles in a largely molten inclusion; (2) nucleation of spinel upon and/or adherence to vapor-melt interfaces, forming spinel shells around vesicles; (3)leakage of vesicles and filling with melt while spinel shells remain largely intact; and (4) crystallization of melt inside shells. This model is similar to one proposed for formation of segregation vesicles, which are partially- to completely-filled vesicles found in some terrestrial basalts. In addition, we interpret framboids (*i.e.*, dense clusters of spinel with little material between grains, found in most inclusions that contain palisade bodies) as polar or near-polar sections through palisade bodies and therefore do not make a genetic distinction between the two features.

INTRODUCTION

Coarse-grained, Ca,Al-rich inclusions (CAIs) found in C3 carbonaceous chondrites typically consist of spinel, melilite, and Ti,Al-rich pyroxene (fassaite), with minor anorthite. All of these phases are among the suite of relatively high-temperature minerals predicted to condense at equilibrium from a cooling gas of solar composition over a range of P^{tot} from 10^{-3} to 10^{-6} atm (*e.g.*, Yoneda and Grossman, 1995). This is strong evidence that CAIs obtained their bulk compositions in the solar nebula, and thus they are very important recorders of early nebular history. However, many CAIs are not pristine gas-solid condensates, having textures, crystallization sequences, and zoning trends within minerals that, along with spherical shapes, indicate that they crystallized from molten droplets. Experimental studies show that the textures observed in natural CAIs are most consistent with crystallization from a partially molten state rather than from a total melt (Stolper and Paque, 1986). Therefore, although it is possible that CAIs underwent multiple melting events, some mineral grains always survived the final one. It is important to identify correctly and to analyze such relict grains in order to learn about the generation of refractory material that immediately predated its host inclusion.

Chains of spinel grains within coarse-grained inclusions were first described by Grossman (1975). The term palisade was first used by Wark and Lovering (1977) in reference to the spinel-rich rim layer enclosing Type B2 CAIs and soon thereafter came to include internal chains, arcs and rings of spinel (Wark *et al.*, 1979). The term palisade body (Wark and Lovering, 1982), in contrast, refers to a spheroidal shell of spinel within a CAI and the material the shell encloses, typically phases found elsewhere in the CAI (melilite, spinel, fassaite, anorthite). Palisades are more common than palisade bodies. In addition, Wark and Lovering (1982) made a distinction between palisade bodies and framboids, the latter being either tightly packed clusters of spinel or round bodies with multiple layers of spinel in their walls, as opposed to the single layers found in palisade bodies. As previously used by El Goresy *et al.* (1979), the term framboid included the palisade bodies of Wark and Lovering (1982).

The origin of palisade bodies is the problem of interest. Wark and Lovering (1982) suggested that palisade bodies are relict mini-CAIs that were captured by their host inclusions. If this is true, then palisade bodies are a very important group of objects. Wark and Lovering (1982) argued that no *in situ* crystallization process could result in palisade body formation and presented isotopic, mineral chemical, and textural arguments that the bodies are exotic to their host CAIs. Wark and Lovering (1982) also argued that framboids, unlike palisade bodies, formed *in situ* by growth in the solid state. El Goresy *et al.* (1979) envisioned formation of framboids (and palisade bodies) either by vapor-solid condensation of spinel onto silicate grains or by formation of open, spheroidal bodies of condensate spinel, which were later infiltrated by vapor or liquid from which silicate minerals crystallized. The purpose of this paper is to reexamine the evidence given by Wark and Lovering (1982) and to present new observations and data, from natural samples and experimental run products, bearing on the origin of palisade bodies and framboids.

ANALYTICAL METHODS

Polished thin sections of CAIs and experimental run products were examined optically and with JEOL JSM-35 and JSM-5800LV scanning electron microscopes. Quantitative wavelength-dispersive analyses were performed with a fully automated Cameca SX-50 electron microprobe operated at 15 kV, with synthetic glasses and natural crystals as standards. Experiments discussed here are from the partitioning study of Simon *et al.* (1996). These were conducted on melts of CAIB composition (after Stolper, 1982). Starting materials (pure oxide and carbonate powders) were dehydrated and decarbonated by heating to 800 °C over a 12 h period and holding at that temperature for 24 h. They were fused by heating to 1550 °C over a 5 h period and were held at that temperature for 24 h, and then quenched. The resulting run products, consisting of nearly vesicle-free glass+spinel, were ground to powders under acetone and stored in a desiccator. For experimental runs, this material was placed on Pt loops in a slurry with polyvinyl alcohol, inserted into a hot (~1100 °C) furnace, heated

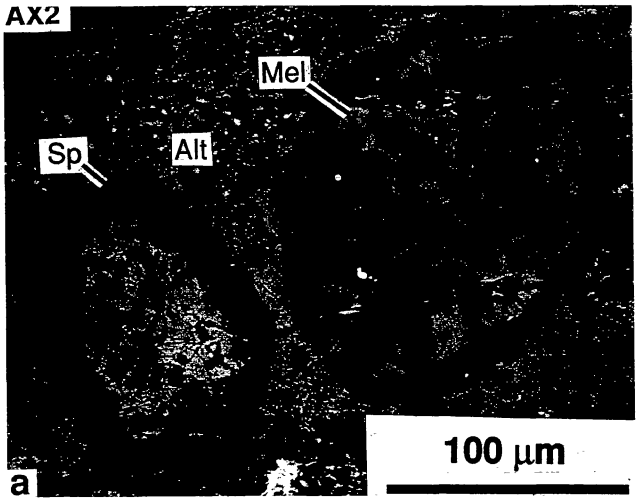

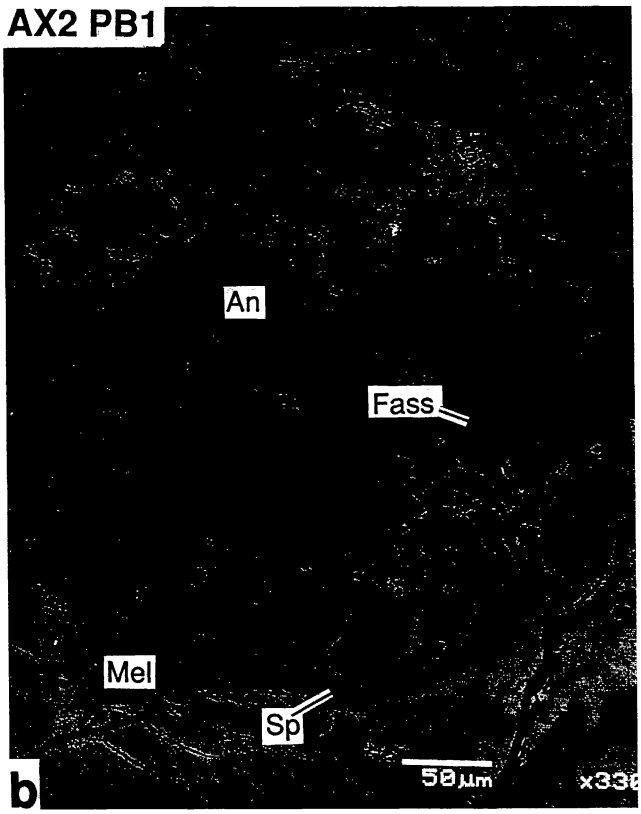

FIG. 1. Backscattered electron images of palisade bodies in Axtell refractory inclusions. (a) Two small bodies in AX2, consisting of melilite and spinel. Some spinel grains in the larger body, on the right, enclose perovskite. (b) A larger fassaite-bearing body, AX2 PB1, in AX2. (c) An anorthite-rich palisade body, AX9 PB1, in AX9. Line AB indicates location of an electron probe traverse in a fassaite grain that is optically continuous across the palisade wall. Abbreviations: Alt = Alteration products; An = Anorthite; Fass = Fassaite; Gr = Grossular; Mel = Melilite; Sp = Spinel.

at 200 °C /h to ~1400 °C (~100 °C below the liquidus), held at that temperature for 3 h, then cooled to 1200 °C at various rates and O fugacities. The runs illustrated in this paper were cooled at 2 °C/h in air and at 20 °C/h at an fO_2 three log units below the iron-wüstite buffer.

OBSERVATIONS

Petrography

This report is inspired by studies of palisade body-rich CAIs from the Axtell C3V chondrite (Simon *et al.*, 1994, 1995) and the discovery of similar features in experimental run products crystallized from melts. Inclusion AX2 is a heavily altered, irregularly shaped Type B2 with ~50% melilite ($Åk_{9-42}$), 15% fassaite with 5.8–16 wt% TiO_2^{tot} (all Ti as TiO_2), 15% spinel, 15% aluminous diopside, and 5% anorthite. Melilite occurs as 5–70 μm-sized grains poikilitically enclosing 5–10 μm-sized spinel grains. Most of the spinel in this inclusion occurs in palisade bodies. At least ten palisade bodies, which range from 50 to 300 μm in diameter, are visible in the section. Fassaite crystals are typically anhedral and ~100 μm across. Inclusion AX9 is also an altered Type B2, with 52% melilite ($Åk_{10-65}$), 30% fassaite (2.8–8.0 wt% TiO_2^{tot}), 14% spinel and 4% anorthite. Melilite, fassaite, and anorthite all occur as anhedral grains up to 500 μm across. In places subhedral melilite grains, 10–20 μm across, are poikilitically enclosed in fassaite or anorthite. Spinel occurs mostly as euhedral grains up to 40 μm across. Both AX2 and AX9 exhibit deep surface re-entrants filled with accretionary rim material.

Several palisade bodies from these inclusions are shown in Fig. 1. Most of the palisade bodies in AX2 consist of only melilite+spinel, like those shown in Fig. 1a. In this otherwise heavily altered inclusion, it appears that the

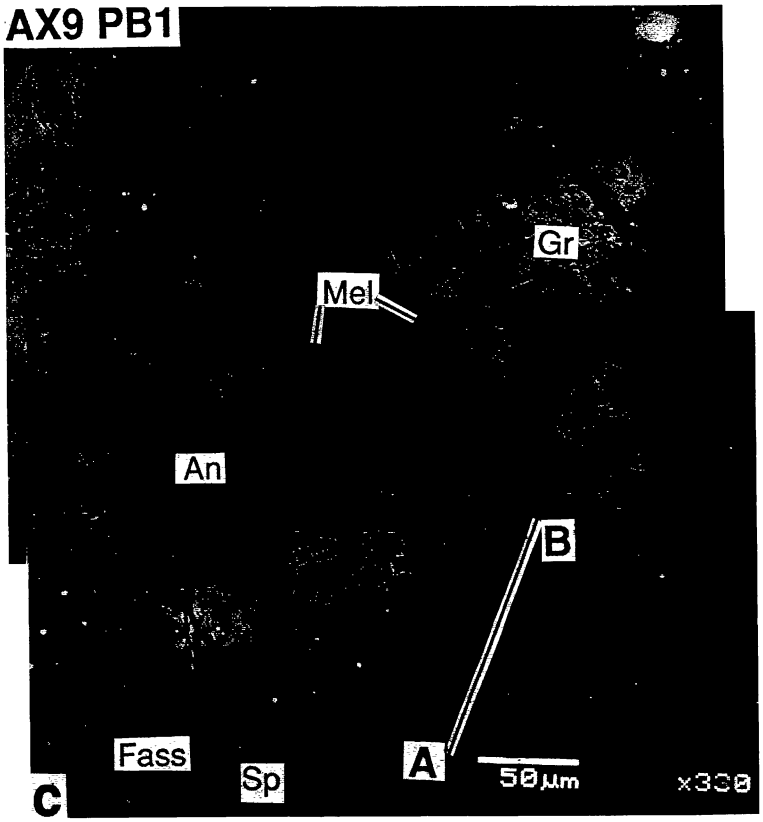

spinel walls of the palisade bodies protected the melilite inside them from alteration to secondary phases such as grossular, anorthite and aluminous diopside. In the palisade bodies shown in Fig. 1a, spinel is subhedral to euhedral, ~10–15 μm across and poikilitically enclosed in melilite. Elsewhere in AX2, there is a larger, 315 μm diameter, more complex palisade body, PB1 (Fig. 1b), that contains anhedral melilite and fassaite, both ~50 μm across and poikilitically enclosing sparse grains of spinel. Note that the palisade wall in most places is one grain thick, as in the illustration by Wark *et al.* (1979) and like several of those shown in photomicrographs by Wark and Lovering (1982; their Figs. 1b and 2). Another rather large body, AX9 PB1, is shown in Fig. 1c. This one is ~350 μm across and is dominated by anorthite, like the one shown in Fig. 2b of Wark and Lovering (1982). Palisade body AX9 PB1 also contains spinel, grossular, fassaite, and minor melilite. The fassaite at the lower right edge of AX9 PB1 is optically continuous with the host fassaite. El Goresy *et al.* (1979) also observed fassaite grains that are optically continuous across palisade body walls.

Chains of spinel, circular structures defined by spinel, and vesicles with adjacent spinel have been observed previously in experimental run products crystallized from melts of an average Type B composition (*e.g.*, Stolper and Paque, 1986). These features were also seen in run products from the experiments of Simon *et al.* (1996), in which melts approximating the CAIB composition of Stolper (1982) were cooled at rates from 2–200 °C/h. All run products in the Simon *et al.* (1996) study contain vesicles, examples of which are illustrated in Fig. 2a,b. In Fig. 2a, four round voids in a glass substrate are shown. Two of the voids are shallow enough that spinel can be seen lining the cavities. Note the concentration of spinel along the former bubble-melt contacts. Most spinel grains in the run products (and in the starting materials) are between 5 and 20 μm across. Four spinel-lined cavities in another run product are shown in Fig. 2b. In addition, at the top center of Fig. 2b (arrow) is a partial ring of spinel filled with glass. Figure 2c shows a circular structure, also filled with glass, in another run product. This structure is bounded by melilite, spinel, and glass. Note the curvature in the shape of the melilite crystal.

Another palisade body, AX9 PB5, containing anorthite, melilite, and fassaite, is shown in Fig. 3a,b. Note how fassaite and anorthite in the host are intergrown with part of the spinel wall (upper center to lower right of Fig. 3b). From the multiple layers of spinel in its wall, this object would be classified as a framboid according to Wark and Lovering (1982), and indeed it is very similar to the one shown in their Fig. 1a. However, because it does consist of a ring of spinel enclosing other phases, we classify the object shown in Fig. 3a as a palisade body and reserve the term framboid for dense clusters of spinel grains, such as that shown in Fig. 3c.

Mineral Chemistry

Fassaite–In Type B inclusions, fassaite crystals are typically zoned from relatively Ti-, Sc-, V-rich, Mg-poor cores to Ti-, Sc-, V-poor and Mg-rich rims (Simon *et al.*, 1991). We analyzed the fassaite in and around several palisade bodies to compare host and palisade body fassaite compositions.

Compositions of fassaite in AX2 PB1 and in its host are similar to each other but are different from typical fassaite from other Type B inclusions from Axtell and Allende. Representative analyses of AX2 fassaite are given in Table 1 and show that both relatively low-Ti fassaite in PB1 and host (columns 1 and 2, respectively) and high-Ti fassaite (columns 3 and 4, respectively) have fairly high

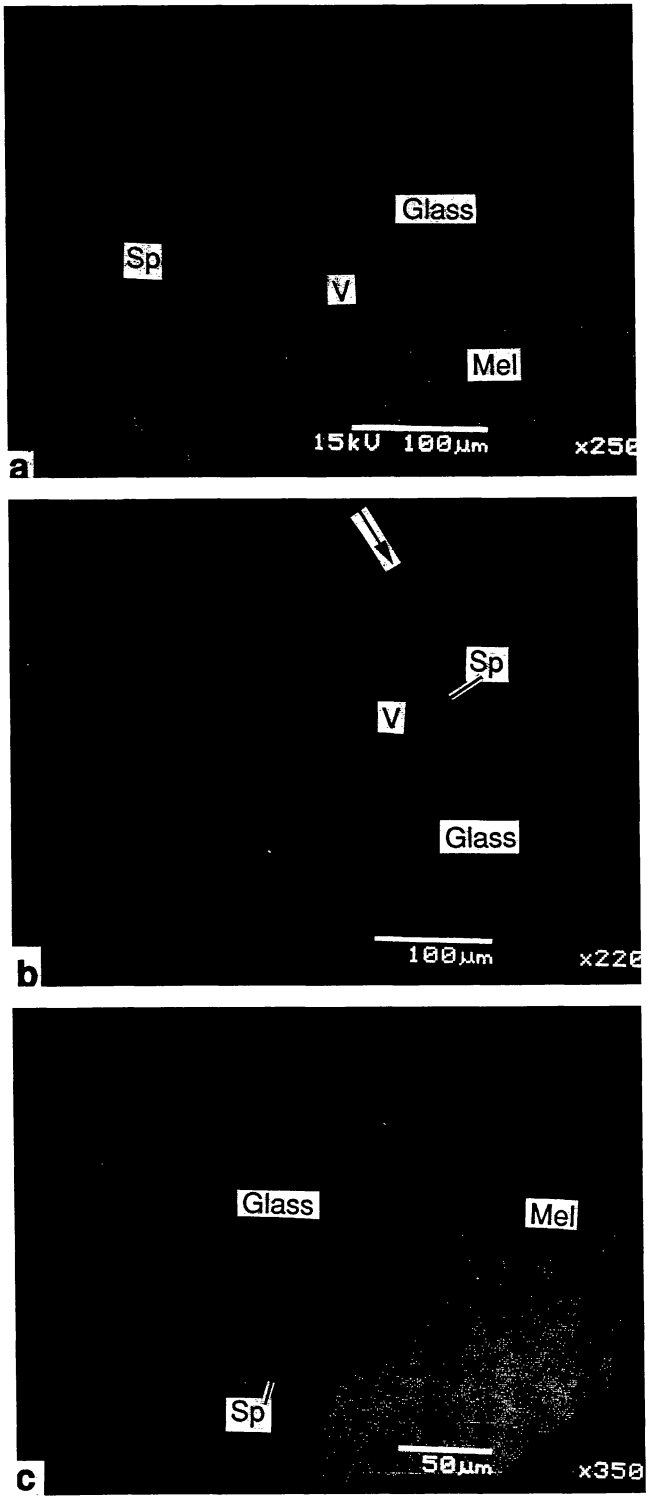

FIG. 2. Backscattered electron images of features observed in experimental run products that crystallized from melts. (a) Spinel-lined, round voids in glass. Run cooled at 2 °C/h in air. (b) Spinel-lined voids, and a partial spinel ring (arrow) which appears to have deflated and filled with melt. Run cooled at 2 °C/h in air. (c) Circular structure outlined by spinel and curved melilite-glass contact. Run cooled at 20 °C/h at three log units below the iron-wüstite buffer. Abbreviations as used previously, except for V = Void.

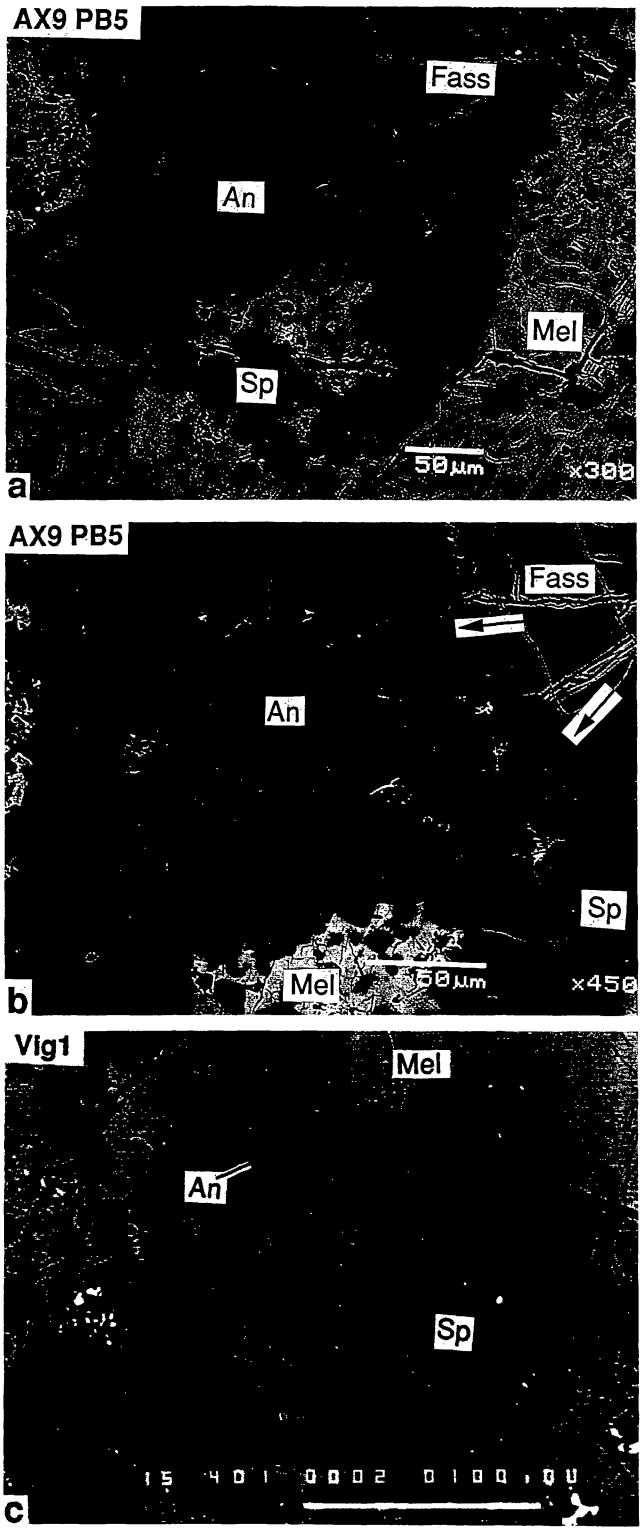

FIG. 3. (a) Palisade body AX9 PB5 which would be classified as a framboid by Wark and Lovering (1982) because of its relatively thick multilayered spinel shell. We consider it a palisade body. (b) Close-up of 3a, showing penetration of host fassaite and anorthite into the spinel wall (arrows). (c) A framboid–a dense cluster of spinel, with little material between grains. Scale bar is 100 μm. Abbreviations as used previously.

TABLE 1. Electron microprobe analyses of fassaite in AX2.

	(1)	(2)	(3)	(4)
MgO	8.21	10.30	8.08	7.95
Al_2O_3	21.00	16.43	19.21	19.32
SiO_2	36.15	39.48	35.47	35.41
CaO	24.92	25.09	25.38	25.07
TiO_2^{tot}	8.39	7.57	11.07	11.39
Sc_2O_3	0.05	0.05	BLD	BLD
V_2O_3	0.68	0.63	0.75	0.72
FeO	0.05	BLD	BLD	BLD
Ti_2O_3	4.18	3.60	6.58	6.93
TiO_2	3.76	3.59	3.95	3.81
TOTAL	99.00	99.17	99.42	99.21
SI	1.355	1.473	1.346	1.342
^{IV}Al	0.645	0.527	0.654	0.658
Tet. sum	2.000	2.000	2.000	2.000
^{IV}Al	0.282	0.195	0.205	0.205
Mg	0.459	0.573	0.457	0.449
Ca	1.000	1.000	1.000	1.000
Fe	0.002	0	0	0
Sc	0.002	0.001	0	0
V	0.019	0.018	0.021	0.020
Ti^{3+}	0.031	0.112	0.205	0.217
Ti^{4+}	0.106	0.101	0.111	0.108
Oct. sum	2.001	2.000	1.999	1.999

(1) = Inside PB1, low-Ti. (2) = Host, low-Ti. (3) = Inside PB1, high-Ti. (4) = Host, high-Ti.
BLD: Below limit of detection of electron microprobe of 0.044 wt% for Sc_2O_3 and 0.042 for FeO.
TiO_2^{tot}: All Ti as TiO_2 (not included in oxide sum). Analyses are normalized to four total cations, including exactly one Ca and two tetrahedral cations (Si and Al) per six O atoms, according to the method of Beckett (1986).

V_2O_3 and very low Sc_2O_3 contents. In Fig. 4, abundances of these three oxides in AX2 fassaite are compared to those in fassaite from three other Axtell Type B inclusions, one Type B2 and two Type B1s. This shows that fassaite in AX2 overlaps fassaite from the other inclusions in TiO_2^{tot} contents, but the former has a higher maximum, ~16 wt%, with higher V_2O_3 and generally much lower Sc_2O_3 contents than fassaite of comparable TiO_2^{tot}. For example, analyses of fassaite in Type B inclusions from both Allende and Axtell show that TiO_2^{tot} and Sc_2O_3 are strongly correlated and fassaite that contains 10–12 wt% TiO_2^{tot} typically has $\geq$0.2 wt% Sc_2O_3, not <0.1%, as is observed in AX2. Note that the distinctive AX2 fassaite is present in both the host and AX2 PB1.

In AX9, in addition to collecting representative analyses in and around AX9 PB1, we conducted a traverse (represented by line AB in Fig. 1c) in the grain that is optically continuous across the palisade wall, from its core, across the palisade wall and into the palisade body. The results are summarized in Table 2 and Figure 5. The crystal is zoned from 7.0 wt% TiO_2^{tot} in its core to 5.9% at the host-palisade contact and from 3.4% just inside AX9 PB1 to 2.5% toward the interior of the palisade body. The V_2O_3 content also drops sharply across the contact from 0.32 to 0.10 wt%. Overall, fassaite in AX9 in the vicinity of PB1 has from 3 to 8 wt% TiO_2^{tot} and that in PB1 has from 2.5 to ~6.5 wt%. Titanium-poor rims on fassaite crystals in the host have compositions that are similar to that of the late, Ti-poor fassaite found in PB1, as can be seen from comparison of the analyses given in the last two columns of Table 2.

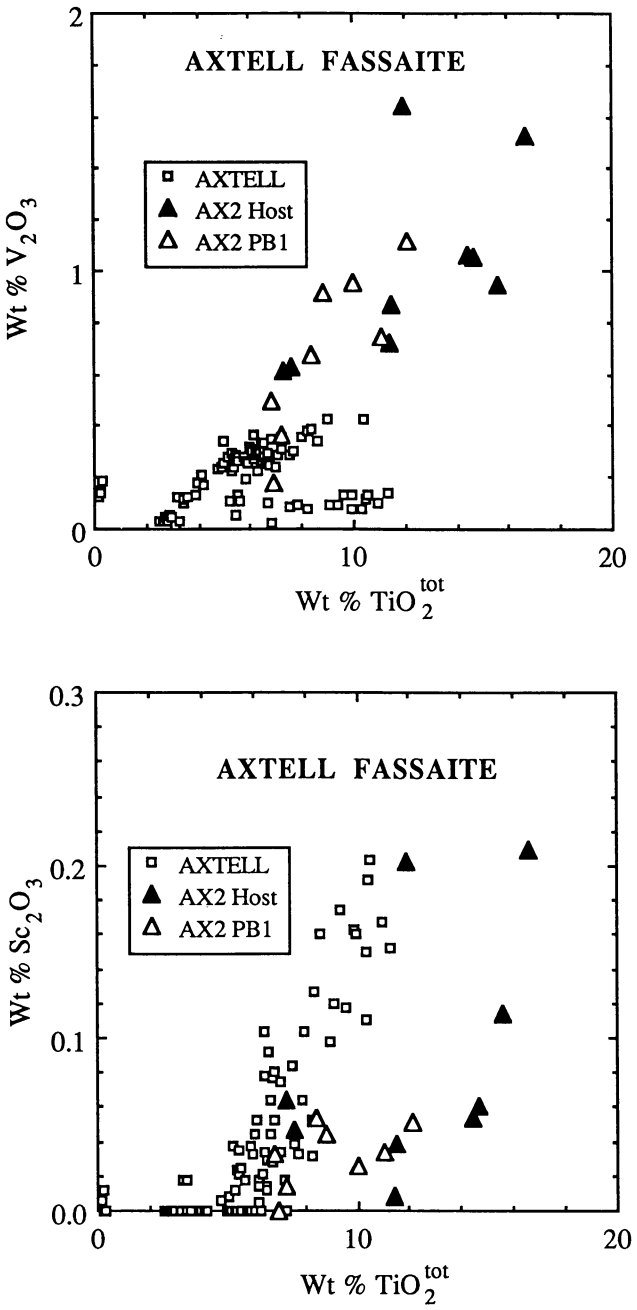

FIG. 4. Abundances of V_2O_3, Sc_2O_3, and TiO_2^{tot} in fassaite in AX2 compared to that in AX2 PB1 and in three other Axtell Type B inclusions (open squares). Compared to that in the other inclusions, fassaite in both AX2 PB1 and the host CAI has high V_2O_3 and TiO_2^{tot} contents but is not correspondingly enriched in Sc_2O_3.

TABLE 2. Electron microprobe analyses of fassaite in AX9.

	(1)	(2)	(3)	(4)	(5)
MgO	9.67	9.78	12.72	13.34	13.20
Al_2O_3	18.30	17.91	12.53	12.00	12.65
SiO_2	39.38	39.72	44.77	45.90	45.75
CaO	25.46	25.21	25.28	25.51	25.70
TiO_2^{tot}	6.99	5.95	3.38	2.69	2.79
Sc_2O_3	0.08	BLD	BLD	BLD	BLD
V_2O_3	0.24	0.32	0.10	0.04	BLD
FeO	BLD	BLD	BLD	BLD	BLD
Ti_2O_3	3.95	3.49	1.55	0.84	0.81
TiO_2	2.65	2.11	1.67	1.76	1.89
TOTAL	99.73	98.54	98.62	99.39	100.00
Si	1.461	1.487	1.655	1.679	1.665
^{IV}Al	0.539	0.513	0.345	0.321	0.335
Tet. sum	2.000	2.000	2.000	2.000	2.000
^{VI}Al	0.261	0.277	0.201	0.197	0.207
Mg	0.534	0.547	0.702	0.728	0.716
Ca	1.000	1.000	1.000	1.000	1.000
Fe	0	0	0	0	0
Sc	0.002	0	0	0	0
V	0.007	0.009	0.003	0.001	0
Ti^{3+}	0.122	0.108	0.048	0.026	0.025
Ti^{4+}	0.074	0.059	0.046	0.048	0.052
Oct. Sum	2.000	2.000	2.000	2.000	2.000

(1) = Host fassaite, 50 μm from PB1. (2) = Host fassaite, just outside wall of PB1. (3) = Just inside wall of PB1. (4) = ~25 μm inside wall of PB1. (5) = Rim of host fassaite.

BLD: Below limit of detection of electron microprobe of 0.044 wt% for Sc_2O_3, 0.031 wt% for V_2O_3, and 0.042 wt% for FeO. Normalization scheme as for Table 1. Ti^{3+} and Ti^{4+} values are not accurate for analyses with <~4 wt% TiO_2^{tot} because of large relative errors associated with small cation abundances.

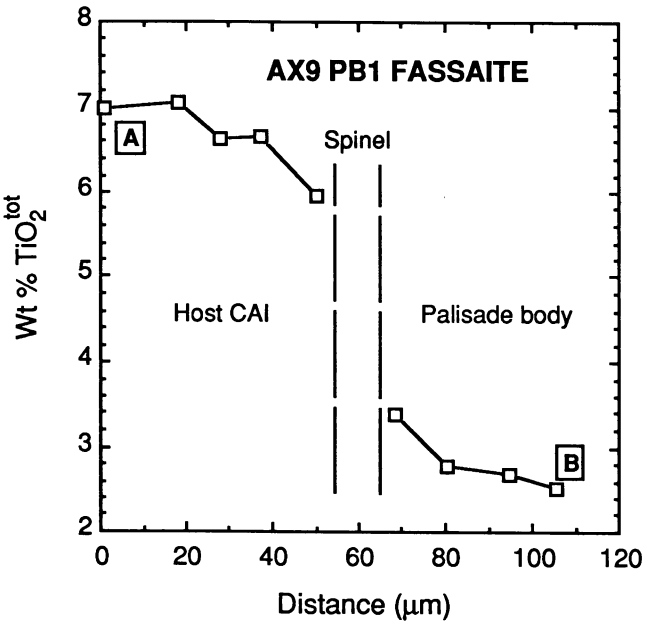

FIG. 5. Results of electron probe traverse along line AB (Fig. 1c), from the host into AX9 PB1. The TiO_2^{tot} of the fassaite inside the palisade wall is much lower than that of the host.

In the cases of both AX2 PB1 and AX9 PB1, the compositions of fassaite in the palisade body and in its host are quite similar to each other. Also, in both samples, the ranges of host fassaite analyses extend to more TiO_2^{tot} - , V_2O_3- and Sc_2O_3-rich (*i.e.*, more primitive) compositions, and those in the palisade bodies extend to TiO_2^{tot} - and V_2O_3- poorer (*i.e.*, more fractionated) compositions.

Melilite–Compositions of melilite in palisade bodies in AX2, AX9 and Vig1 (Simon and Grossman, 1991) are compared to those in their host inclusions in Fig. 6. Of 15 palisade bodies analyzed, 14 have ranges completely within, or extending to more åkermanitic compositions than, the ranges observed in their host CAIs. In the remaining case, there is some compositional overlap between palisade body and host melilite, but the range of the former extends to slightly more gehlenitic compositions than the latter. Some palisade bodies exhibit very narrow ranges in composition, while others exhibit very wide ranges. In most cases, the most gehlenitic melilite within a palisade body is found just inside the palisade wall, with the relatively magnesian melilite tending to occur closer to the core of the palisade body. Where more than one analysis could be obtained on a single crystal, the results indicate that the melilite grains within palisade bodies are normally zoned, with åkermanite contents increasing toward crystal rims. In many cases, as was observed by Wark and Lovering (1982), melilite just inside a palisade wall is very close in composition to that just outside of the palisade wall. Not including two large Type B1 inclusions enclosed in Type A material found by Wark and Lovering (1982), those workers showed melilite compositions for three palisade bodies and their hosts. One palisade body, with $Åk_{65}$, is much less gehlenitic than its host ($Åk_{47}$); another, with $Åk_{20-27}$, is more gehlenitic than its host ($Åk_{26-36}$); and, in the third case, palisade body and host have quite similar but unusual melilite compositions: $Åk_{82-85}$ and $Åk_{84-87}$, respectively.

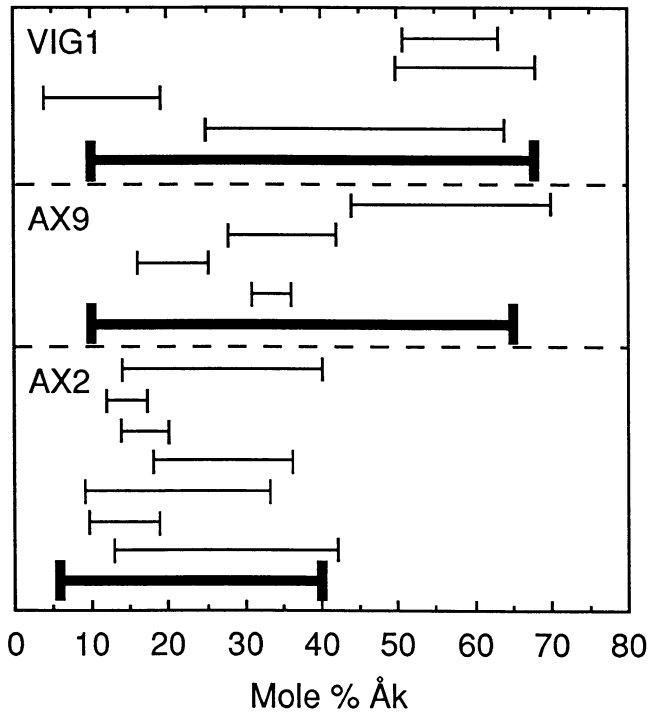

FIG. 6. Ranges of melilite compositions observed in 15 palisade bodies in three inclusions (thin lines), compared to the ranges observed in the host inclusions (heavy lines). In most cases, palisade body melilite falls within the range observed in the host.

These compositions are on the Mg-rich side of the minimum in the åkermanite-gehlenite system (Osborn and Schairer, 1941); so, although it is slightly more gehlenitic, the melilite in the palisade body also has a more evolved composition than that in the host.

DISCUSSION

The Model

For reasons given below, we believe that our data and observations and some of those of Wark and Lovering (1982) are generally not consistent with origin of palisade bodies by capture of exotic objects and are best explained by an *in situ* formation process in which (1) vesicles form in molten CAIs; (2) spinel nucleates upon and/or collects against vapor-melt interfaces and sticks to them, forming shells around the bubbles; (3) vesicles break during crystallization and the escaping vapor is replaced with melt while spinel shells remain largely intact; and (4) melt inside shells solidifies *in situ*. The process is analogous to that believed responsible for the formation of segregation vesicles found in some basalts and interpreted by Smith (1967) and Anderson *et al.* (1984) as early-formed vesicles that were partially to completely filled with melt while the flow was still partially molten, with their original shapes preserved by a rigid network of crystals through which melt could flow.

In the experiments considered here, air between the grains of the starting powders was either trapped by the resulting melt or dissolved in it and later exsolved, forming the vesicles. During crystallization, dissolved air would behave incompatibly, becoming concentrated and eventually saturated in the melt. In natural CAIs, vesicles could have formed from interstitial nebular gas that was trapped during melting of precursor grain aggregates. Formation of CAIs most likely occurred at total gas pressures between 10^{-3} and 10^{-6} atm. For these conditions, we estimate the vapor pressure over a metastable CAI melt would be about four orders of magnitude lower than the ambient pressure. The nebular gas is therefore the most likely candidate for the filling of bubbles in molten CAIs.

Evidence for *In Situ* Formation of Palisade Bodies

Wark and Lovering (1982) considered and rejected several ways that palisade bodies could have formed *in situ*. We agree with their rejection of (a) liquid immiscibility, (b) devitrification, (c) subsolidus reactions, (d) nucleation upon relict grains, and (e) remelting in the interiors of Type B inclusions. They also ruled out nucleation on bubbles because, in their experiments, rounded voids that were infiltrated by melt were not associated with spinel. As shown in Fig. 2, our observations of experimental run products differ from those of Wark and Lovering (1982). Like Stolper and Paque (1986), we found spinel-lined voids to be rather common, weakening the Wark and Lovering (1982) argument against this mode of formation. Stolper and Paque (1986) reported that, in their experimental run products, spinel was concentrated on Pt loops and on the surfaces of charges as well as on bubbles. This indicates a general tendency of spinel to nucleate upon or at least stick to certain liquid/vapor or liquid/solid interfaces. The feature in Fig. 2c suggests that bubble shapes can be preserved by the arrangement of spinel crystals. Note also in Fig. 2c the concave melilite-glass contact, which attests to the strength of the meniscus against impinging crystallization. We interpret glass-filled rings of spinel, such as the kidney-shaped one at the top of Fig. 2b, as deflated, melt-filled bubbles. A similar feature, AX9 PB2 (Fig. 7), consists of a partial ring of spinel with what appears to be a flap frozen in the process of opening, possibly by the sudden escape of gas during bubble breakage. Unless it is a fortuitous

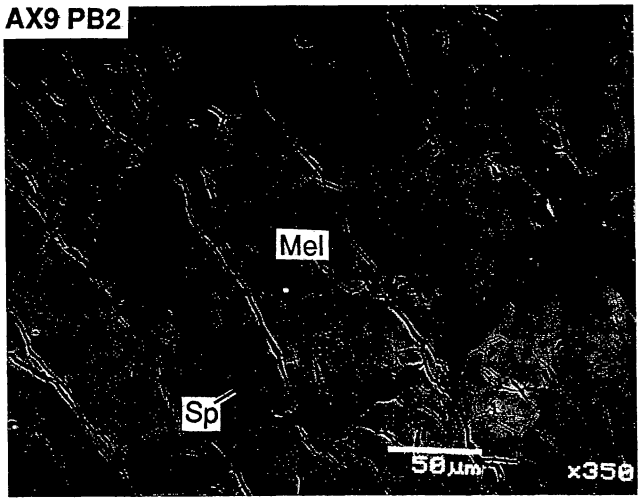

FIG. 7. Palisade body AX9 PB2 that froze while breaking. Note "flaps" of spinel adjacent to the opening in the right side of the shell. Abbreviations as used previously.

arrangement of crystals unrelated to the rest of the ring, the flap consists of grains that moved in tandem during opening of the ring, reflecting flow outward through the spinel wall.

If, as suggested by Wark and Lovering (1982), palisade bodies were solid objects captured by their hosts, these observations would require that AX9 PB2 melted after capture. This, in turn, requires the host CAI to have been very hot long enough to melt the palisade body to the point where some liquid could flow out and open the flap. Melilite inside AX9 PB2 is $Åk_{16-25}$, so unless PB2 originally contained relatively magnesian melilite, melted, and exchanged melt with the host, melting after incorporation would require that the host was hot enough to melt melilite more gehlenitic than $Åk_{25}$. From the experiments of Stolper (1982), this would imply that the inclusion was hotter than ~1400 °C. This is at the upper end of the range of temperatures from which Type B CAIs most likely crystallized (Stolper and Paque, 1986), requiring that capture occurred at or near the peak temperature in the crystallization history of AX9. In addition, this scenario also requires that the spinel shell of PB2 not be completely destroyed while enclosing molten melilite in a molten host without the support of a vapor-melt meniscus. A much more straightforward interpretation is that AX9 PB2, analogous to the open ring found in the synthetic melt (Fig. 2b), originally was the location of a bubble that broke, pushing a section of the spinel wall outward, and the plane of the thin section fortuitously sampled the site of this rupture. As the vapor escaped, it was replaced with melt, possibly through another rupture not seen in the section. The features shown in Figs. 2 and 7 are very strong evidence for *in situ* formation of palisade bodies.

It is interesting to note that inclusions AX9 and AX2 both have deep, rounded re-entrants in their rims, which likely resulted from the escape of gas bubbles as the molten inclusions were solidifying. A vesicular refractory inclusion with deep re-entrants, ALVIN, was found in Allende by MacPherson *et al.* (1981), who suggested that there is a connection between re-entrants and vesicles. However, ALVIN is a forsterite-bearing inclusion that lacks spinel; so, its vesicles are not spinel-lined. Most inclusions are not vesicular, but we examined backscattered electron photomosaics of 18 coarse-grained inclusions (16 Type B and 2 Type A) from Allende, Axtell and Vigarano to see if there is a relationship between re-entrants in the inclusion margins and the presence of palisade bodies within the inclusions. The results are suggestive of a relationship. Six of the inclusions, including AX2 and AX9, have re-entrants and, of these, five contain palisade bodies. Of the twelve that do not have re-entrants, only three have palisade bodies. Thus, while it is possible to have palisade bodies without re-entrants and *vice versa*, most (5/6) of the inclusions with re-entrants have palisade bodies, and most (9/12) of those without re-entrants also do not have palisade bodies.

Another argument used by Wark and Lovering (1982) against the origin of palisade bodies by the filling of vesicles was the observation that voids in their experimental run products were filled with late liquid, with relatively low melting temperatures, which conflicts with their claim that most palisade bodies have higher melting points than their hosts. Of the three palisade body–host pairs described in detail by Wark and Lovering (1982), however, only one palisade body, with $Åk_{20-27}$, has melilite that is more gehlenitic and therefore has a higher melting point than its host ($Åk_{26-36}$). In addition, as Fig. 6 shows, of our 15 cases, only one contains melilite that is more gehlenitic than any observed in the host, and melilite compositions in all 15 palisade bodies exhibit considerable overlap with those of their hosts. Thus, out of a total of 18 palisade bodies analyzed, there are just two in which the most gehlenitic melilite is outside of the range observed in the host, in both cases by only ~6 mol%. It is certainly possible that with further analysis such gehlenitic melilite could be found in the hosts as well. Note that the vesicles can fill at any point and trap any liquid, from early to late, consistent with the wide range of assemblages observed in palisade bodies. Some may trap very early liquids, which crystallize gehlenitic melilite, while others, such as two of the palisade bodies we have shown from AX9, PB1 (Fig. 1c) and PB5 (Figs. 3a, b), which contain anorthite and low-Ti fassaite ± Mg-rich melilite, trapped late-stage melts. The tendency of vesicles to fill with late-stage melts is not a good argument against our model for *in situ* formation of palisade bodies.

Segregation vesicles are also typically invaded by relatively fractionated melts (Anderson *et al.*, 1984), despite their high viscosities. Using the empirical method of Shaw (1972), Anderson *et al.* (1984) estimated the viscosities of the basaltic melts that filled vesicles in the samples they studied to have been 10^5–10^6 P at 1000–1100 °C, the approximate temperature range over which the filling occurred. For comparison, we used the method of Shaw (1972) to calculate a viscosity of ~10 P at 1275 °C for the composition of glass from a run product on an average Type B CAI composition (Stolper, 1982). As the run product contains 55% glass, the composition of the glass ought to be representative of the residual melt after 45% crystallization. Its viscosity is much lower than those of the materials in the terrestrial segregation vesicles, probably because the CAI melt has a much higher molar (MgO + CaO)/(Al_2O_3 + SiO_2) ratio than fillings of the segregation vesicles. Because the latter material could flow, so too could a residual melt in a partially molten CAI. Therefore, high melt viscosities are not likely to hinder vesicle-filling in CAIs.

Wark and Lovering cited "abrupt changes in texture across palisades" as evidence against *in situ* formation. We also observe sharp textural contrasts between some palisade bodies and their hosts, such as that seen in Fig. 1c, in which AX9 PB1 contains less spinel and fassaite and more anorthite than the immediate host. We do not believe that this rules out *in situ* formation. If a vesicle filled during the late stages of crystallization, as AX9 PB1 did, it is highly unlikely

that the infiltrating melt would have the same composition or solidify in the same texture as the host, which crystallized earlier, at a higher temperature. Segregation vesicles also typically exhibit sharp textural contrast between host and vesicle filling, the former typically crystalline and the latter typically glass or devitrified glass (Smith, 1967; Anderson *et al.*, 1984). In spite of the contrast in texture between AX9 PB1 and its host, some of the fassaite in it is optically continuous with that of the host, which is strong evidence for *in situ* formation of the palisade body. One such grain is zoned, with TiO_2 decreasing from its core toward the palisade wall and within the palisade body from the wall toward the interior, with a gap of ~2.5 wt% TiO_2^{tot} between the fassaite just outside the palisade wall and that just inside (Table 2). The compositional discontinuity is best explained by inward epitaxial growth of the AX9 PB1 fassaite on the host fassaite from a liquid that had continued to evolve after crystallization of the host fassaite stopped against the palisade wall or meniscus, as melilite in our run product (Fig. 2c) did. Fassaite growth continued after the late-stage liquid leaked into a vesicle. If PB1 were exotic, then the optical continuity of the fassaite would have to be explained by nucleation of the host fassaite on that in AX9 PB1, which would require that TiO_2^{tot} of the fassaite increased as it grew, which is opposite to normal zoning. The penetration of fassaite and anorthite into the wall of AX9 PB5 (Fig. 3b) is also not consistent with the latter being captured as an intact, solid object.

An absence of palisade-like structures in terrestrial rocks strengthened the argument of Wark and Lovering (1982) that palisade bodies did not form by conventional igneous or even metamorphic processes. Igneous rocks in which spinel is the liquidus phase are extremely rare; so, we would not expect to find such structures in terrestrial rocks. Although segregation vesicles are not spinel-lined, they do provide strong evidence for the basic process envisioned here: filling of early-formed vesicles after the partially molten host became rigid enough to preserve the vesicle shape. In the case of terrestrial rocks, this is thought to require ~50% crystallization (Anderson *et al.*, 1984) but, in CAIs, it could occur with much lower degrees of crystallization due to the early formation of spinel shells around vesicles.

Examination of the Evidence for Exotic Formation of Palisade Bodies

The evidence given by Wark and Lovering (1982) in favor of an exotic origin of palisade bodies is not compelling and can also be reconciled with an *in situ* origin. Specific points that they raised that we have not already addressed are discussed below.

Magnesium Isotopic Differences between Palisade Body and Host–This evidence consisted of one ion probe analysis of anorthite in a palisade body in Allende Type B2 inclusion TS21, reported by Hutcheon and Steele (1980). Hutcheon (1982) showed that on a plot of $^{26}Mg/^{24}Mg$ *vs.* $^{27}Al/^{24}Mg$, analyses of anorthite from the interior of this inclusion plot on a line with a slope equal to the initial $^{26}Al/^{27}Al$ ratio of $4.6 \pm 0.3 \times 10^{-5}$, whereas analyses of anorthite from the exterior (outermost ~200 μm) of the inclusion define a line with a slope of $2.3 \pm 0.2 \times 10^{-5}$. The linear arrays are consistent with *in situ* decay of ^{26}Al and a younger, probably disturbed, age for the exterior anorthite relative to that in the interior. The palisade anorthite yielded the only analysis of an interior anorthite to plot off the interior anorthite isochron, falling between the trends of the interior and exterior anorthite. Wark and Lovering (1982) interpreted this anorthite as exotic, isotopically distinct material that was added to the inclusion and did not equilibrate with the host. If, however, it is the case that this anorthite has remained undisturbed and its isotopic composition reflects its true age, then based on its lower inferred initial $^{26}Al/^{27}Al$ ratio (Hutcheon and Steele, 1980; Hutcheon, 1982), the palisade body would be younger than its host, which is inconsistent with the palisade body being preexisting material that was incorporated by the host inclusion while the latter was still forming. It seems more likely that the isotopic composition of the palisade anorthite was affected by heating and/or alteration, which can cause isotopic exchange (Podosek *et al.*, 1991), but to a lesser extent than were those of the exterior grains in the inclusion.

Kennedy *et al.* (1990) analyzed spinel in a palisade in the mantle of Allende Type B1 3655A and found that its Mg is isotopically heavier than the bulk Mg of the inclusion. Goswami *et al.* (1994) also found Mg isotopic evidence for relict spinel in a Type B CAI. This leads to the conclusions that some of the spinel predates the last melting event and that the inclusion precursor was isotopically heterogeneous (Kennedy *et al.*, 1990), but it does not prove that the palisade body predates the inclusion. It could have formed *in situ,* by accumulation of both relict and non-relict spinel grains against a bubble/melt meniscus.

Differing Mineral Chemistries of Palisade Bodies and Hosts–Although Wark and Lovering (1982) considered such mineral chemical differences as evidence of an exotic origin for palisade bodies, they did acknowledge the possibility that such differences could be created *in situ.* Two palisade bodies, one from Allende (Wark and Lovering, 1982) and one from Vigarano (Simon and Grossman, 1991), contain the most gehlenitic melilite of their inclusions. Accounting for these objects with our model would require, assuming sampling were representative, that these palisade bodies either trapped relict melilite or formed from melt from which the first melilite in the inclusion crystallized. In addition, the spinel in the Vigarano palisade body is slightly more V_2O_3-rich than that elsewhere in the inclusion (Simon and Grossman, 1991); so, *in situ* formation would probably require relict spinel as well. This is not a problem as textures of Type B inclusions are not consistent with crystallization of total melts, and spinel and gehlenitic melilite are the phases most likely to be relict. Wark and Lovering (1982) also reported a palisade body in Allende Type B inclusion 110,A in which metal and sulfide grains are much rarer and more Ni-rich than those in the host. This is, admittedly, difficult to reconcile with *in situ* formation, although it is possible that the palisade body could have contained Ni-rich immiscible melt globules that were rare and not sampled elsewhere in the section. However, this same palisade body contains extremely magnesian melilite, $Åk_{82-85}$, as does the host inclusion ($Åk_{84-87}$). Despite the differences in opaque mineral populations between palisade body and host, the observations are much more consistent with *in situ* than with exotic formation of the palisade body because it is very unlikely that this inclusion, with a very rare melilite composition, by random capture incorporated a palisade body with virtually the same, rare composition. Similarly, it seems an unlikely coincidence that AX2 PB1 contains V_2O_3-rich, Sc_2O_3-poor fassaite like that in the host. Overall, the similarities of palisade and host mineral compositions are more striking than the differences.

Palisade Bodies in Hosts of Different CAI Type–This evidence consists of two, large (several millimeter) "Type B1 palisade bodies" inside "Type A hosts". In these objects, outer melilite-rich zones (Type A parts) enclose inner melilite-rich zones (mantles of

Type B1 parts), with the two zones separated by spinel palisades. The Type A parts were thought by Wark and Lovering (1982) to be condensates containing exotic objects that crystallized from liquids. For one of these objects (Egg 3), however, Wark and Lovering (1982) gave evidence of continuity between the Type A and Type B1 parts based on overlap of melilite compositions and minor element contents of spinel, metal, and sulfide grains. Thus, another way of looking at these objects is as true Type B1 inclusions whose thick melilite mantles are traversed by spinel chains which may represent detached rim layers that foundered during crystallization of the melilite mantles. Unlike Wark and Lovering (1982), we do not consider the B1 parts of these inclusions to be analogous to the palisade bodies that are much smaller than their CAI hosts.

The Resemblance of Palisade Bodies to Mini-CAIs–Wark and Lovering (1982) cite several similarities and differences between palisades and the spinel rims found on CAIs. They noted that both range in morphology from chains of discrete single crystals to continuous ribbons in which faces on individual spinel crystals cannot be discerned. Wark and Lovering (1977) noted that chains are more common in the rims of Type B2 inclusions and ribbons are more commonly found on Type A and B1 inclusions, although the correlation is not perfect (Wark *et al.*, 1979). From the textural resemblance of the spinel shells of some palisade bodies to the spinel rims on some inclusions, Wark and Lovering (1982) considered the spinel shells analogous to rims and thus palisade bodies analogous to mini-CAIs, thereby supporting their contention that palisade bodies were independent objects that were later incorporated by their hosts. We find that among palisade bodies, chains of discrete spinel crystals are much more common than ribbons of intergrown spinel regardless of palisade body mineralogy. In addition, palisade bodies generally lack the perovskite, hibonite, and nearly pure gehlenite (<~10 mol% Åk) found in or just inside of the spinel rim layers of both Type A (MacPherson and Grossman, 1979; Wark and Lovering, 1980) and Type B (Wark and Lovering, 1977; Davis *et al.*, 1992) inclusions. Furthermore, if we consider the overall mineralogy of palisade bodies, and not just the textures of spinel shells, we see that many palisade bodies, especially anorthite-dominated ones, do not have minerals in modal proportions that are typical of the major CAI types; some palisade bodies do not even contain melilite (Wark and Lovering, 1982). Thus, many palisade bodies do not resemble common CAIs and contain mineral assemblages that are less refractory than would be expected for early-forming, proto-CAIs. Arguments for the origin of palisade bodies as exotic materials based on their identity with known, independent objects are weakened with the recognition that palisade bodies are not really so similar to CAIs.

Branched Palisades–Wark and Lovering (1982) observed branches, or forks, in spinel rim layers of inclusions and palisade bodies and considered this another way in which the structures are analogous. One way in which they envisioned the formation of branched palisades was by breakage of the spinel shell of a palisade body, followed by extrusion of some liquid, and crystallization of spinel at the outer margin of the extruded melt, all occurring prior to incorporation of the palisade body into a CAI. Branched palisades could also form *in situ*, for example, by breakage, foundering and lateral displacement of part of the initial spinel crust of a partially molten palisade body within a partially molten CAI. Branched palisades do not provide strong evidence for exotic formation of palisade bodies.

Framboids

Given that palisade bodies are most likely three-dimensional shells of spinel, and not two-dimensional rings as they appear to be in thin section, it stands to reason that they will not always be sectioned representatively. Off-center sections of palisade bodies will undersample the "cores" and appear to have thicker shells and smaller diameters than would equatorial sections of the corresponding bodies. The object shown in Fig. 3a,b may be an example of such an off-center section of a palisade body. In the extreme case, polar sections will sample only spinel, resulting in spinel clumps or clusters with little material between grains appearing in thin section. This theory leads to the prediction, assuming random distribution of the objects within inclusions, that inclusions will generally either contain both palisade bodies and framboids, or neither, and this is essentially what we find. We examined eight inclusions that contain palisade bodies and, of these, six have framboids, while, of ten inclusions that do not have palisade bodies, only one has framboids. If they were unrelated there should be no correlation between inclusions with palisade bodies and those with framboids. We see no reason to make a genetic distinction between framboids and palisade bodies.

CONCLUSIONS

We have considered petrographic observations and quantitative analyses of palisade bodies in light of two models for their origin: (a) they are early-formed, proto-CAIs unrelated to, and captured by, their present host inclusions (Wark and Lovering, 1982); and (b) they formed *in situ* within partially molten host CAIs as a result of nucleation of spinel upon and/or its adherence to vesicle-melt interfaces, which gave rise to vesicles with spinel shells. During crystallization, vapor escaped from the vesicles, and melt entered and crystallized inside the spinel shells. Our observations of (1) spinel-lined vesicles and circular, glass-filled structures outlined by spinel and melilite in experimental run products; (2) a partially formed palisade body in a CAI; (3) a fassaite grain optically continuous across a palisade wall; and (4) mineral compositions in palisade bodies that mimic those in the host, such as the V-rich fassaite in AX2, the late fassaite in AX9, and the extremely magnesian melilite in 110, A (Wark and Lovering, 1982), are most consistent with, and strong evidence for an *in situ* origin for most palisade bodies. If we assume that early-formed, proto-CAIs should have higher melting temperatures than their hosts, then only the rare palisade bodies with melilite that is more gehlenitic than any in their hosts are candidate proto-CAIs. We also conclude that it is most likely that framboids are polar or near-polar sections through palisade bodies and see no need for a genetic distinction between the two features.

Acknowledgments–We thank A. T. Anderson, Jr. for bringing segregation vesicles to our attention, F. Richter for helpful discussions and for providing details about the experiments on CAI melts, and A. M. Davis for helpful discussions and for help with the SEM. Comments by A. Kennedy led to improvements in the text. The Axtell samples were generously loaned by the Field Museum. This work was supported by NASA through grant NAGW-3340, and funding is gratefully acknowledged.

Editorial handling: H. Nagahara

REFERENCES

ANDERSON A. T., JR., SWIHART G. H., ARTIOLI G. AND GEIGER C. A. (1984) Segregation vesicles, gas filter-pressing, and igneous differentiation. *J. Geol.* **92,** 55–72.

BECKETT J. R. (1986) The origin of calcium-, aluminum-rich inclusions from carbonaceous chondrites: An experimental study. Ph.D. thesis, University of Chicago. 373 pp.

DAVIS A. M., SIMON S. B. AND GROSSMAN L. (1992) Melilite composition trends during crystallization of Allende Type B1 refractory inclusion melts (abstract). *Lunar Planet. Sci.* **23,** 281–282.

EL GORESY A., NAGEL K. AND RAMDOHR P. (1979) Spinel framboids and fremdlinge in Allende inclusions: Possible sequential markers in the early history of the solar system. *Proc. Lunar Planet. Sci. Conf.* **10th,** 833–850.

GOSWAMI J. N., SRINIVASAN G. AND ULYANOV A. A. (1994) Ion microprobe studies of Efremovka CAIs: I. Magnesium isotope composition. *Geochim. Cosmochim. Acta* **58,** 431–448.

GROSSMAN L. (1975) Petrography and mineral chemistry of Ca-rich inclusions in the Allende meteorite. *Geochim. Cosmochim. Acta* **39,** 433–454.

HUTCHEON I. D. (1982) Ion probe magnesium isotopic measurements of Allende inclusions. *Amer. Chem. Soc. Symp. Ser.* **176,** 95–128.

HUTCHEON I. D. AND STEELE I. M. (1980) Mineralogy and Mg isotopic composition of Type B2 inclusions from Leoville and Allende (abstract). *Lunar Planet. Sci.* **11,** 496–498.

KENNEDY A. K., BECKETT J. R. AND HUTCHEON I. D. (1990) Trace element and isotopic constraints on the formation and crystallization of a Type B1 CAI from Allende (abstract). *Lunar Planet. Sci.* **21,** 621–622.

MACPHERSON G. J. AND GROSSMAN L. (1979) Melted and non-melted coarse-grained Ca-, Al-rich inclusions in Allende (abstract). *Meteoritics* **14,** 479–480.

MACPHERSON G. J., GROSSMAN L., ALLEN J. M. AND BECKETT J. R. (1981) Origin of rims on coarse-grained inclusions in the Allende meteorite. *Proc. Lunar Planet. Sci. Conf.* **12B,** 1079–1091.

OSBORN E. F. AND SCHAIRER J. F. (1941) The ternary system pseudo-wollastonite-åkermanite-gehlenite. *Am. J. Sci.* **239,** 715–763.

PODOSEK F. A., ZINNER E. K., MACPHERSON G. J., LUNDBERG L. L., BRANNON J. C. AND FAHEY A. J. (1991) Correlated study of initial $^{87}Sr/^{86}Sr$ and Al-Mg isotopic systematics and petrologic properties in a suite of refractory inclusions from the Allende meteorite. *Geochim. Cosmochim. Acta* **55,** 1083–1110.

SHAW H. R. (1972) Viscosities of magmatic silicate liquids: An empirical method of prediction. *Am. J. Sci.* **272,** 870–893.

SIMON S. B. AND GROSSMAN L. (1991) Petrography of a suite of refractory inclusions from the Leoville, Efremovka and Vigarano carbonaceous chondrites (abstract). *Lunar Planet. Sci.* **22,** 1261–1262.

SIMON S. B., GROSSMAN L. AND DAVIS A. M. (1991) Fassaite composition trends during crystallization of Allende Type B refractory inclusion melts. *Geochim. Cosmochim. Acta* **55,** 2635–2655.

SIMON S. B., GROSSMAN L. AND WACKER J. F. (1994) Unusual refractory inclusions from a CV3 chondrite found near Axtell, Texas (abstract). *Lunar Planet. Sci.* **25,** 1275–1276.

SIMON S. B., GROSSMAN L., CASANOVA I., SYMES S., BENOIT P., SEARS D. W. G. AND WACKER J. F. (1995) Axtell, a new CV3 chondrite find from Texas. *Meteoritics* **30,** 42–46.

SIMON S. B., DAVIS A. M., RICHTER F. M. AND GROSSMAN L. (1996) Experimental investigation of the effect of cooling rate on melilite/liquid distribution coefficients for Sr, Ba and Ti in Type B refractory inclusion melts (abstract). *Lunar Planet. Sci.* **27,** 1201–1202.

SMITH R.E. (1967) Segregation vesicles in basaltic lava. *Am. J. Sci.* **265,** 696–713.

STOLPER E. (1982) Crystallization sequences of Ca-Al-rich inclusions from Allende: An experimental study. *Geochim. Cosmochim. Acta* **46,** 2159–2180.

STOLPER E. AND PAQUE J. M. (1986) Crystallization sequences of Ca-Al-rich inclusions from Allende: The effects of cooling rate and maximum temperature. *Geochim. Cosmochim. Acta* **50,** 1785–1806.

WARK D. A. AND LOVERING J. F. (1977) Marker events in the early evolution of the solar system: Evidence from rims on Ca-Al-rich inclusions in carbonaceous chondrites. *Proc. Lunar. Sci. Conf.* **8th,** 95–112.

WARK D. A. AND LOVERING J. F. (1980) Second thoughts about rims (abstract). *Lunar Planet. Sci.* **11,** 1211–1213.

WARK D. A. AND LOVERING J. F. (1982) Evolution of Ca-Al-rich bodies in the earliest solar system: Growth by incorporation. *Geochim. Cosmochim. Acta* **46,** 2595–2607.

WARK D. A., WASSERBURG G. J. AND LOVERING J. F. (1979) Structural features of some Allende coarse-grained Ca-Al-rich inclusions: Chondrules within chondrules? (abstract). *Lunar Planet. Sci.* **10,** 1292–1294.

YONEDA S. AND GROSSMAN L. (1995) Condensation of CaO-MgO-Al_2O_3-SiO_2 liquids from cosmic gases. *Geochim. Cosmochim. Acta* **59,** 3413–3444.